PHYSICAL REVIEW D **82,** 034513 (2010)

Spontaneous symmetry breaking in a two-doublet lattice Higgs model

Randy Lewis
Department of Physics and Astronomy, York University, Toronto, Ontario, Canada M3J 1P3

R. M. Woloshyn
TRIUMF, 4004 Wesbrook Mall, Vancouver, British Columbia, Canada V6T 2A3
(Received 4 June 2010; published 31 August 2010)

An SU(2) lattice gauge theory with two doublets of complex scalar fields is considered. All continuous symmetries are identified and, using the nonperturbative methods of lattice field theory, the phase diagram is mapped out by direct numerical simulation. Two-doublet models contain phase transitions that separate qualitatively distinct regions of the parameter space. In some regions global symmetries are spontaneously broken. For some special choices of the model parameters, the symmetry-breaking order parameter is calculated. The pattern of symmetry breaking is verified further through observation of Goldstone bosons.

DOI: 10.1103/PhysRevD.82.034513 PACS numbers: 11.15.Ha, 11.15.Ex, 11.30.Fs, 11.30.Qc

I. MOTIVATION

The Higgs mechanism lies at the heart of the standard model of electroweak interactions, where it is implemented efficiently through a single SU(2) doublet of scalar fields. The scalar doublet's mass-squared term is chosen to be negative and analysis of small fluctuations around the minimum of the classical scalar potential leads to the conclusion that the weak gauge bosons acquire appropriate masses. This standard model is generally viewed as the low-energy effective theory for something more complete, and in many extensions multiple scalar doublets appear. An old, but still useful, review of the Higgs mechanism where multiple doublets participate may be found in [1].

A different specific implementation of two scalar doublets is the inert doublet model of [2] (see also [3]). Instead of taking both scalar doublets to have nonzero vacuum expectation values (vevs), the inert doublet model assumes that there is a phase in which one doublet has a vanishing vev while the other does not. This provides some additional motivation for examining the possible phases of two-doublet models in a more general way.

In this work we use lattice field theory to study some features of the Higgs model with two doublets. Lattice field theory provides a nonperturbative method for studying non-Abelian gauge theories. An important difference of the lattice formulation from the continuum is the use of the gauge field link variable, which, taking values in the gauge group, allows calculations to be done without gauge fixing [4]. This has the immediate consequences that expectation values of non-gauge-invariant operators vanish and that the gauge symmetry cannot be spontaneously broken [5,6]. It also implies that physical states of the system are gauge-invariant composite objects.[1] These are features shared by lattice Higgs models and lattice QCD.

[1]A view of the electroweak theory along these lines has been espoused by Fröhlich *et al.* [7].

Soon after lattice field theory was developed it was applied to Higgs models [8–12]. Lattice simulations of the one-doublet model were carried out extensively in the 1980s and early 1990s with applications to the study of the phase diagram and basic particle spectrum [13–19], bounds on the scalar (Higgs) mass [20] and the study of the electroweak finite-temperature phase transition [21–24]. In addition, bounds on the Higgs boson mass have been obtained from simulations with Higgs-Yukawa theories that omit all gauge interactions [25–32].

An early observation [8,11] was that the SU(2) lattice Higgs model with a single doublet of scalar fields in the fundamental representation should actually have only a single phase. There are regions in parameter space, sometimes named the confinement region and the Higgs region, which have a qualitatively different mass spectrum. In most of the parameter space these regions are separated by a phase transition. However, there is a corner of parameter space where the transition disappears and through which the confined and Higgs regions can be analytically connected. There is no (local) order parameter and no broken symmetry to distinguish the two regions.

With regard to the spectrum, the low-lying states of the one-doublet SU(2) lattice Higgs model consist of a scalar singlet and a triplet of vector bosons. These states are massive in all regions of the parameter space. Note that the Goldstone bosons which emerge in an intermediate stage of the standard perturbative treatment of the Higgs mechanism and which are subsequently absorbed into the longitudinal components of the massive vector bosons do not appear in the nonperturbative lattice calculation.

Dramatic qualitative changes may occur when additional scalar doublets are present in the theory. In particular, there are two regions of the phase diagram which are now completely separated by a phase transition throughout parameter space [33]. One might expect that these phases are distinguished by having different global symmetries, and if so, there will be corresponding order parameters.

There may be regions of the parameter space where global symmetries are spontaneously broken and Goldstone bosons are present in the spectrum of physical states. In the present work, we study a gauge theory with two scalar doublets using numerical lattice simulations in which this scenario is realized.

The lattice action is defined in Sec. II and its continuous symmetries are discussed. Section III presents the numerical simulations used to determine vacuum expectation values that produce a map of the phase diagram of this two-doublet lattice Higgs model. Section IV describes the methods used to search for spontaneous symmetry breaking. The symmetry-breaking order parameter is calculated and the Goldstone bosons that accompany each broken generator are identified. Section V contains a summary.

II. LATTICE ACTION AND SYMMETRIES

This study is based on an action for an SU(2) gauge theory with two complex scalar doublets where each doublet has its own global SU(2) symmetry.[2] On a spacetime lattice, the action can be written as

$$S = \sum_x (\mathcal{L}_g[U] + \mathcal{L}_1[\Phi_1, U] + \mathcal{L}_2[\Phi_2, U] + \mathcal{L}_{12}[\Phi_1, \Phi_2]), \tag{1}$$

where

$$\mathcal{L}_g[U] = \frac{\beta}{2} \sum_{\mu=1}^{4} \sum_{\nu=1}^{4} \left(1 - \frac{1}{2} \mathrm{Tr}[U_\mu(x) U_\nu(x+\mu) \times U_\mu^\dagger(x+\nu) U_\nu^\dagger(x)]\right), \tag{2}$$

$$\mathcal{L}_n[\Phi_n, U] = \Phi_n^\dagger(x)\Phi_n(x) + \lambda_n(\Phi_n^\dagger(x)\Phi_n(x) - 1)^2 - \kappa_n \sum_{\mu=1}^{4} (\Phi_n^\dagger(x+\mu) U_\mu^\dagger(x) \Phi_n(x) + \Phi_n^\dagger(x) U_\mu(x) \Phi_n(x+\mu)), \tag{3}$$

$$\mathcal{L}_{12}[\Phi_1, \Phi_2] = 2\lambda_{12} \Phi_1^\dagger(x)\Phi_1(x)\Phi_2^\dagger(x)\Phi_2(x). \tag{4}$$

$U_\mu(x)$ is the gauge field and $\Phi_n(x)$ is a complex scalar doublet. Notice that the couplings λ_1 and λ_2 multiply more than just quartic terms, in contrast to common practice in the continuum. Likewise the normalization of the scalar fields $\Phi_n(x)$ follows conventions of lattice field theory rather than continuum conventions, and thus we show hopping parameters κ_n instead of quadratic coefficients μ_n^2. The classical relationship between the lattice and continuum notations may be found in [12]. All parameters and fields in the lattice action are dimensionless.

The 4 degrees of freedom in a complex doublet,

$$\Phi_n(x) = \begin{pmatrix} a(x) + ib(x) \\ c(x) + id(x) \end{pmatrix}, \tag{5}$$

can also be expressed as a matrix,

$$\varphi_n(x) = \begin{pmatrix} c(x) - id(x) & a(x) + ib(x) \\ -a(x) + ib(x) & c(x) + id(x) \end{pmatrix}, \tag{6}$$

which is a more convenient notation in some contexts. In this notation, the scalar terms in the Lagrangian become

$$\mathcal{L}_n[\varphi_n, U] = \frac{1}{2} \mathrm{Tr}[\varphi_n^\dagger(x)\varphi_n(x)] + \lambda_n \left(\frac{1}{2} \mathrm{Tr}[\varphi_n^\dagger(x)\varphi_n(x)] - 1\right)^2 - \kappa_n \sum_{\mu=1}^{4} \mathrm{Tr}[\varphi_n^\dagger(x) U_\mu^\dagger(x) \varphi_n(x+\mu)], \tag{7}$$

$$\mathcal{L}_{12}[\varphi_1, \varphi_2] = \frac{\lambda_{12}}{2} \mathrm{Tr}[\varphi_1^\dagger(x)\varphi_1(x)] \mathrm{Tr}[\varphi_2^\dagger(x)\varphi_2(x)]. \tag{8}$$

This action has one local continuous symmetry, namely, the gauge symmetry defined by

$$U_\mu(x) \to R_g(x) U_\mu(x) R_g^\dagger(x+\mu), \tag{9}$$

$$\Phi_1(x) \to R_g(x)\Phi_1(x), \tag{10}$$

$$\Phi_2(x) \to R_g(x)\Phi_2(x), \tag{11}$$

where $R_g(x)$ is an element of SU(2). The action has two global continuous symmetries, one for each scalar doublet, which will be referred to as intradoublet symmetries. They are defined by

$$\varphi_1(x) \to \varphi_1(x) R_1, \tag{12}$$

$$\varphi_2(x) \to \varphi_2(x) R_2, \tag{13}$$

where R_1 and R_2 are elements of SU(2). Finally, the action acquires an additional global continuous symmetry in the special case of ($\kappa_1 = \kappa_2$, $\lambda_1 = \lambda_2 = \lambda_{12}$). This additional symmetry will be called the interdoublet symmetry, and it is defined by

$$\begin{pmatrix} \Phi_1(x) \\ \Phi_2(x) \end{pmatrix} \to R_{12} \begin{pmatrix} \Phi_1(x) \\ \Phi_2(x) \end{pmatrix}, \tag{14}$$

where R_{12} is an element of U(2).

It is important to understand the intricate connection between the interdoublet and intradoublet symmetries. To elucidate this connection, use the explicit form

$$R_n = \begin{pmatrix} e^{-i\alpha_n} \cos\gamma_n & e^{i\beta_n} \sin\gamma_n \\ -e^{-i\beta_n} \sin\gamma_n & e^{i\alpha_n} \cos\gamma_n \end{pmatrix} \tag{15}$$

[2]This restricts the form of the allowed quartic coupling terms. Terms allowed by gauge symmetry but which break the generic SU(2) × SU(2) global symmetry are excluded here although they may be present in phenomenological applications [1].

for $n = 1$ or 2 which gives

$$\Phi_n(x) \to \cos\gamma_n e^{i\alpha_n}\Phi_n(x) + \sin\gamma_n e^{i\beta_n}\Phi_{cn}(x), \quad (16)$$

$$\Phi_{cn}(x) \to \cos\gamma_n e^{-i\alpha_n}\Phi_{cn}(x) - \sin\gamma_n e^{-i\beta_n}\Phi_n(x), \quad (17)$$

where $\Phi_{cn}(x) \equiv i\tau_2\Phi_n^*(x)$. The interdoublet symmetry can be parametrized in a similar fashion, but it is convenient to have it act on

$$\begin{pmatrix} \Phi_1(x) \\ \Phi_{c2}(x) \end{pmatrix}$$

rather than on

$$\begin{pmatrix} \Phi_1(x) \\ \Phi_2(x) \end{pmatrix},$$

giving

$$\begin{pmatrix} \Phi_1(x) \\ \Phi_{c2}(x) \end{pmatrix} \to \begin{pmatrix} e^{i\delta_{12}}e^{-i\alpha_{12}}\cos\gamma_{12} & e^{i\delta_{12}}e^{i\beta_{12}}\sin\gamma_{12} \\ -e^{i\delta_{12}}e^{-i\beta_{12}}\sin\gamma_{12} & e^{i\delta_{12}}e^{i\alpha_{12}}\cos\gamma_{12} \end{pmatrix} \times \begin{pmatrix} \Phi_1(x) \\ \Phi_{c2}(x) \end{pmatrix}. \quad (18)$$

Now we can combine Eqs. (16)–(18) to write down the transformation of our scalar fields under an arbitrary global transformation:

$$\Phi_1 \to \cos\gamma_{12}e^{i(\delta_{12}-\alpha_{12})}(\cos\gamma_1 e^{i\alpha_1}\Phi_1 + \sin\gamma_1 e^{i\beta_1}\Phi_{c1}) + \sin\gamma_{12}e^{i(\delta_{12}+\beta_{12})}(\cos\gamma_2 e^{-i\alpha_2}\Phi_{c2} - \sin\gamma_2 e^{-i\beta_2}\Phi_2), \quad (19)$$

$$\Phi_{c2} \to \cos\gamma_{12}e^{i(\delta_{12}+\alpha_{12})}(\cos\gamma_2 e^{-i\alpha_2}\Phi_{c2} - \sin\gamma_2 e^{-i\beta_2}\Phi_2) - \sin\gamma_{12}e^{i(\delta_{12}-\beta_{12})}(\cos\gamma_1 e^{i\alpha_1}\Phi_1 + \sin\gamma_1 e^{i\beta_1}\Phi_{c1}). \quad (20)$$

Finally we notice that two of the ten parameters (i.e. the α_i, β_i, γ_i and δ_i) are redundant. Let us choose the eight independent parameters to be γ_1, γ_2, γ_{12},

$$\rho_1 \equiv \alpha_1 + \delta_{12} - \left(\frac{\alpha_{12}+\beta_{12}}{2}\right), \quad (21)$$

$$\omega_1 \equiv \beta_1 + \delta_{12} - \left(\frac{\alpha_{12}+\beta_{12}}{2}\right), \quad (22)$$

$$\rho_2 \equiv \alpha_2 - \delta_{12} - \left(\frac{\alpha_{12}+\beta_{12}}{2}\right), \quad (23)$$

$$\omega_2 \equiv \beta_2 - \delta_{12} - \left(\frac{\alpha_{12}+\beta_{12}}{2}\right), \quad (24)$$

$$\theta \equiv \frac{\beta_{12}-\alpha_{12}}{2}. \quad (25)$$

When expressed in terms of the new parameters, Eqs. (19) and (20) become

$$\Phi_j \to e^{i\theta}[\cos\gamma_{12}(\cos\gamma_j e^{i\rho_j}\Phi_j + \sin\gamma_j e^{i\omega_j}\Phi_{cj}) + \sin\gamma_{12}(\cos\gamma_k e^{-i\rho_k}\Phi_{ck} - \sin\gamma_k e^{-i\omega_k}\Phi_k)], \quad (26)$$

$$\Phi_{cj} \to e^{-i\theta}[\cos\gamma_{12}(\cos\gamma_j e^{-i\rho_j}\Phi_{cj} - \sin\gamma_j e^{-i\omega_j}\Phi_j) - \sin\gamma_{12}(\cos\gamma_k e^{i\rho_k}\Phi_k + \sin\gamma_k e^{i\omega_k}\Phi_{ck})], \quad (27)$$

where $(j, k) = (1, 2)$ or (2,1). We now recognize the continuous global symmetries as

$$\mathrm{SU}(2) \times \mathrm{SU}(2) \times \mathrm{U}(1) \times \mathrm{U}(1) \quad \text{if } (\kappa_1 = \kappa_2, \lambda_1 = \lambda_2 = \lambda_{12}) \text{ is true,} \quad (28)$$

where the parameters of the four factors are respectively $(\rho_1, \omega_1, \gamma_1)$, $(\rho_2, \omega_2, \gamma_2)$, γ_{12} and θ. Of course whenever $(\kappa_1 = \kappa_2,\ \lambda_1 = \lambda_2 = \lambda_{12})$ is not valid, the continuous global symmetries are just the intradoublet ones,

$$\mathrm{SU}(2) \times \mathrm{SU}(2) \quad \text{if } (\kappa_1 = \kappa_2, \lambda_1 = \lambda_2 = \lambda_{12}) \text{ is not true,} \quad (29)$$

which amounts to choosing $\gamma_{12} = 0$. The parameter θ is then redundant, so neither of the U(1) symmetries remains whenever $(\kappa_1 = \kappa_2,\ \lambda_1 = \lambda_2 = \lambda_{12})$ is not valid.

To conclude this section, return to the defining action of Eq. (1) and consider the special case of fixed-length scalar fields,

$$\Phi_1^\dagger(x)\Phi_1(x) = \Phi_2^\dagger(x)\Phi_2(x) = 1. \quad (30)$$

In this limit, the theory is independent of parameters λ_1, λ_2 and λ_{12}. With only the κ_i parameters remaining, the fixed-length theory bears a notable resemblance to QCD-like theories and has been studied in some detail [34–36].

III. THE PHASE DIAGRAM

In numerical simulations, each scalar or gauge field is evaluated using a combination of heatbath and overrelaxation updates combined with an accept-reject step that accounts for non-Gaussian terms in the action. The algorithm contains a parameter that is tuned to produce a good acceptance rate. Details of the algorithm can be found in [33]; for more extensive discussions of algorithms see [37–39].

Phase transitions are readily identified, on a lattice with N sites, by scanning through parameter space and computing simple observables such as the average plaquette

$$\frac{1}{2N}\sum_{x,\mu<\nu}\mathrm{Tr}U_\mu(x)U_\nu(x+\mu)U_\mu^\dagger(x+\nu)U_\nu^\dagger(x), \quad (31)$$

Polyakov loops

$$\frac{1}{2N}\sum_x \mathrm{Tr}\prod_n U_4(x+n\hat{4}), \quad (32)$$

gauge-invariant links, where $(i, j) = (1, 1)$ or (1,2) or (2,2),

$$L_{ij} \equiv \frac{1}{N}\sum_x (\Phi_i^\dagger(x) U_\mu(x) \Phi_j(x+\mu) + \text{h.c.}), \tag{33}$$

and the mixed vev

$$\frac{1}{N}\sum_x |\Phi_1^\dagger(x)\Phi_2(x)|^2. \tag{34}$$

Note that the mixed gauge-invariant link ($i \neq j$) and mixed vev do not preserve the intradoublet symmetries, and recall that Polyakov loops are order parameters for confinement in the pure gauge theory and are sometimes used to provide a nonrigorous definition of confinement in the one-doublet SU(2)-Higgs model [40]. Figs. 1 and 2 show examples of scanning through $\kappa_1 = \kappa_2$ values while holding β fixed in the fixed-length theory. For the mixed invariant link and mixed vev, statistical errors (not shown) scale inversely with $\sqrt{N}\sqrt{\#\text{configurations}}$ at small κ but they scale inversely with $\sqrt{\#\text{configurations}}$ at large κ. This behavior is indicative of the spontaneous breaking of intradoublet symmetries. The Polyakov loops are affected by the phase transition at $\beta = 4$ but not at $\beta = 0.25$, suggesting that the phase transition separates a confinement region from a

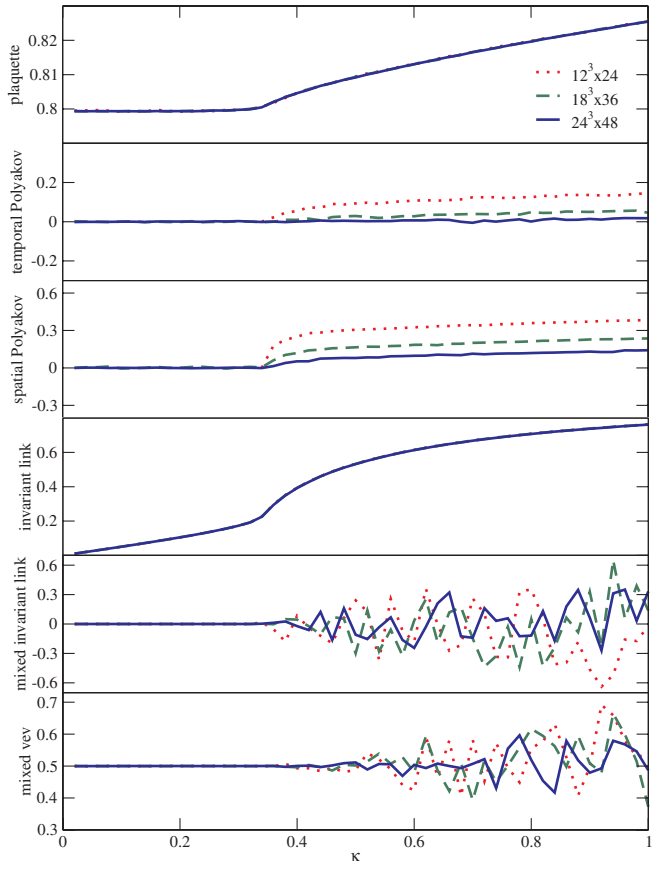

FIG. 1 (color online). Indications of the phase transition from a variety of observables for the fixed-length theory at $\beta = 4.0$. Three different lattice sizes are shown.

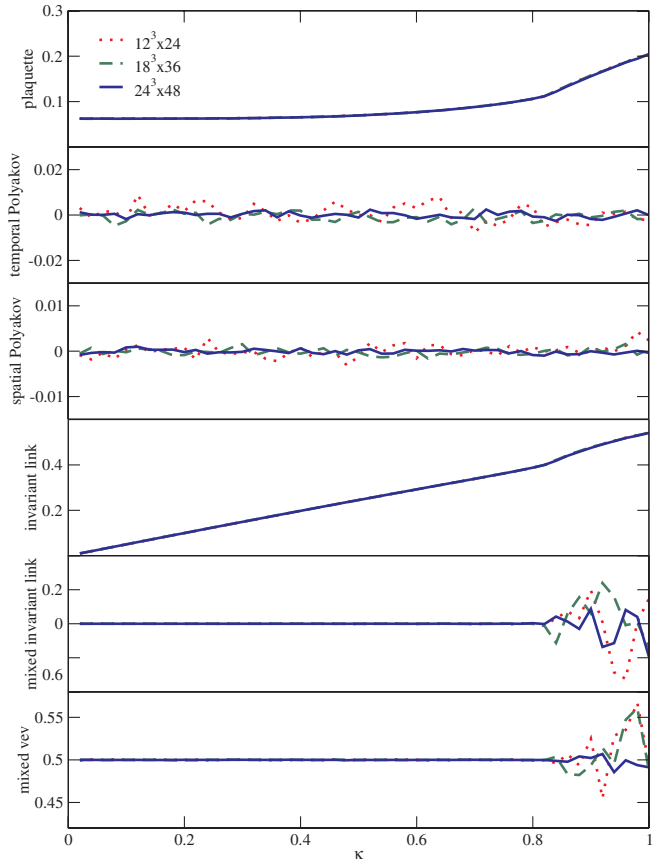

FIG. 2 (color online). Indications of the phase transition from a variety of observables for the fixed-length theory at $\beta = 0.25$. Three different lattice sizes are shown.

Higgs region at large β only. This is precisely how the confinement/Higgs transition melts away in the one-doublet SU(2)-Higgs model as well [8].

Figs. 1 and 2 also indicate that the location of the phase transition is rather insensitive to the size of the lattices employed. The average plaquette and gauge-invariant link undergo a qualitative change at the phase transition for all β, and in practice the gauge-invariant link is a convenient first diagnostic when searching for the phase transition.

The phase diagram for the fixed-length theory is shown for three different β values in Fig. 3. Since large β corresponds to weak gauge coupling, it is not surprising that one finds two orthogonal phase transitions: one separating the Higgs and confinement phases of the first scalar field (and therefore essentially independent of κ_2 in the figure) and the other for the second scalar field (essentially independent of κ_1). This divides the κ_1, κ_2 plane into four regions but these are not four separate phases as is evident from results at smaller β. At $\beta = 2$ the phase transitions affect one another near their mutual crossing point, and for $\beta = 1$ only a single phase transition is evident. The corresponding data for $\lambda_1 = \lambda_2 = 1$, with $\lambda_{12} = 0$, are given in Fig. 4.

As is clear from Figs. 3 and 4, there is always a single phase transition in a theory with degenerate scalar fields

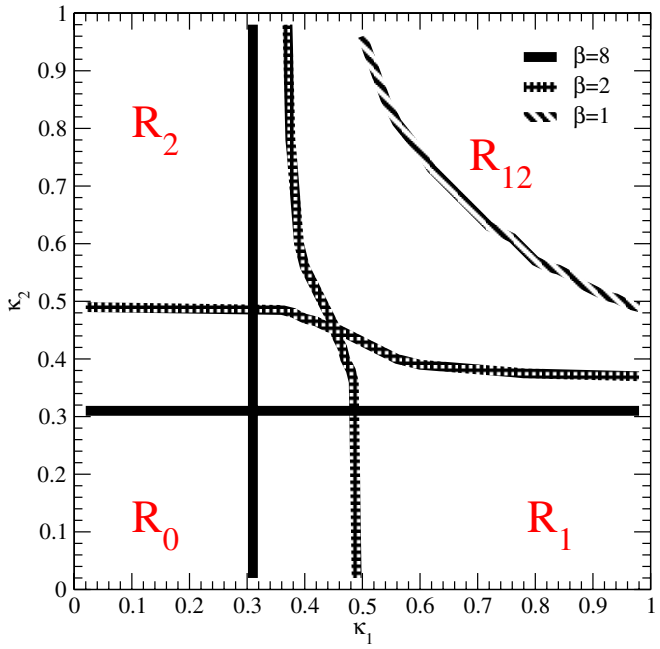

FIG. 3 (color online). Phase diagram for the fixed-length theory as computed for three different β values on 16^4 lattices. R_{12} is the broken-symmetry region where L_{12} of Eq. (33) is nonzero. All other regions are analytically connected at small β but quantitatively distinguished at larger β by finding large L_{11} values in region R_1, large L_{22} values in region R_2, and small values for both L_{11} and L_{22} in region R_0.

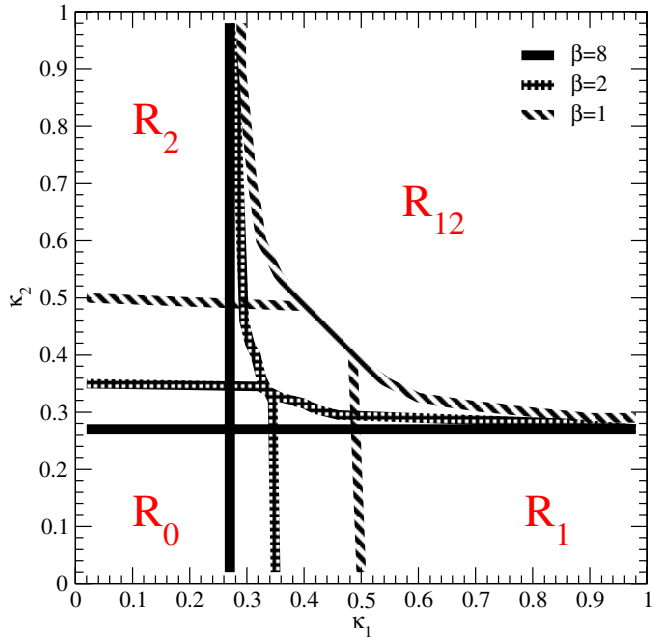

FIG. 4 (color online). Phase diagram for the theory with $\lambda_1 = \lambda_2 = 1$ and $\lambda_{12} = 0$, as computed for three different β values on 16^4 lattices. R_{12} is the broken-symmetry region where L_{12} of Eq. (33) is nonzero, region R_1 has large L_{11}, region R_2 has large L_{22}, and region R_0 has small L_{11} and L_{22}.

($\kappa_1 = \kappa_2$), but nondegenerate fields typically have more. Choosing $\kappa_1 = 2\kappa_2$ for definiteness, it is not clear from Fig. 3 which observables display a qualitative change at which phase boundaries, so this information is provided in Figs. 5 and 6. The Polyakov loops are zero in the R_0 region but with no clear transition for small β, while the observables that mix Φ_1 and Φ_2 display their qualitative change at the R_{12} boundary. These results suggest that the R_0 region be viewed as the confinement region, and the R_{12} region is the phase of broken intradoublet symmetry.

All of the simulations discussed so far have used $\lambda_{12} = 0$, but it is interesting to explore nonzero values of this parameter since the lattice action has an interdoublet symmetry when ($\kappa_1 = \kappa_2$, $\lambda_1 = \lambda_2 = \lambda_{12}$). The effect on the phase diagram due to variation of λ_{12} is plotted in Fig. 7 for the case of $\beta = 8.0$, $\lambda_1 = \lambda_2 = 1$. The two phase transition lines, which were essentially straight and orthogonal at $\lambda_{12} = 0$ in Fig. 4, bend toward one another at large hopping parameters as λ_{12} is increased. This pinching of the phase of broken intradoublet symmetry continues until that phase is reduced to a single line at $\lambda_{12} = 1$. That line runs along $\kappa_1 = \kappa_2$ which is precisely where the extra interdoublet symmetry is manifest in the lattice action.

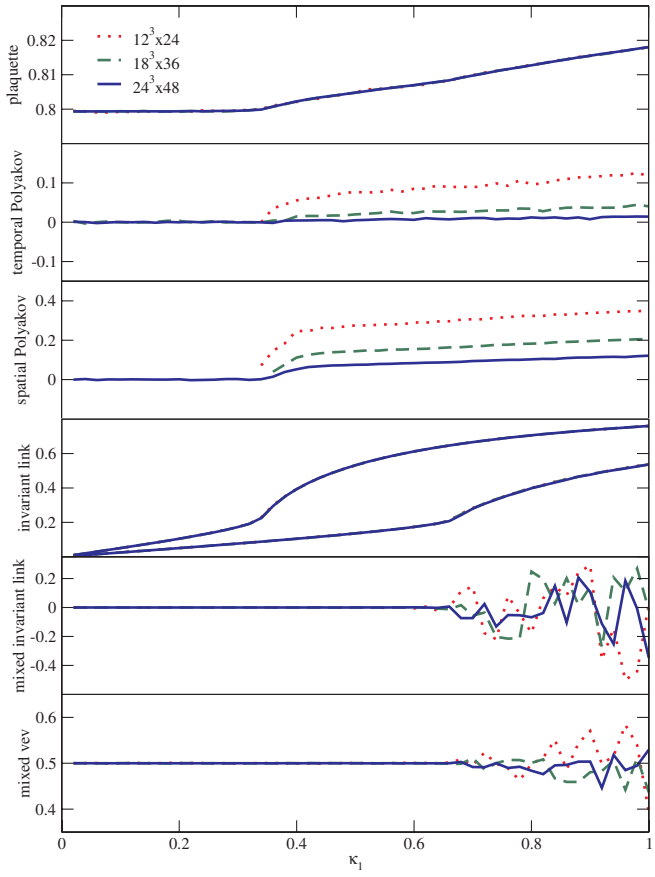

FIG. 5 (color online). Indications of the phase transition from a variety of observables for the fixed-length theory at $\beta = 4.0$ with $\kappa_1 = 2\kappa_2$. Three different lattice sizes are shown.

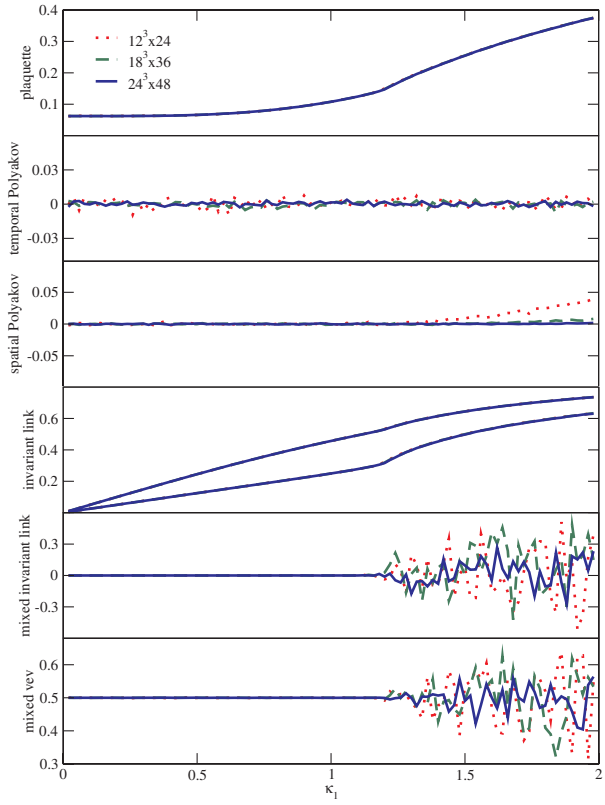

FIG. 6 (color online). Indications of the phase transition from a variety of observables for the fixed-length theory at $\beta = 0.25$ with $\kappa_1 = 2\kappa_2$. Three different lattice sizes are shown.

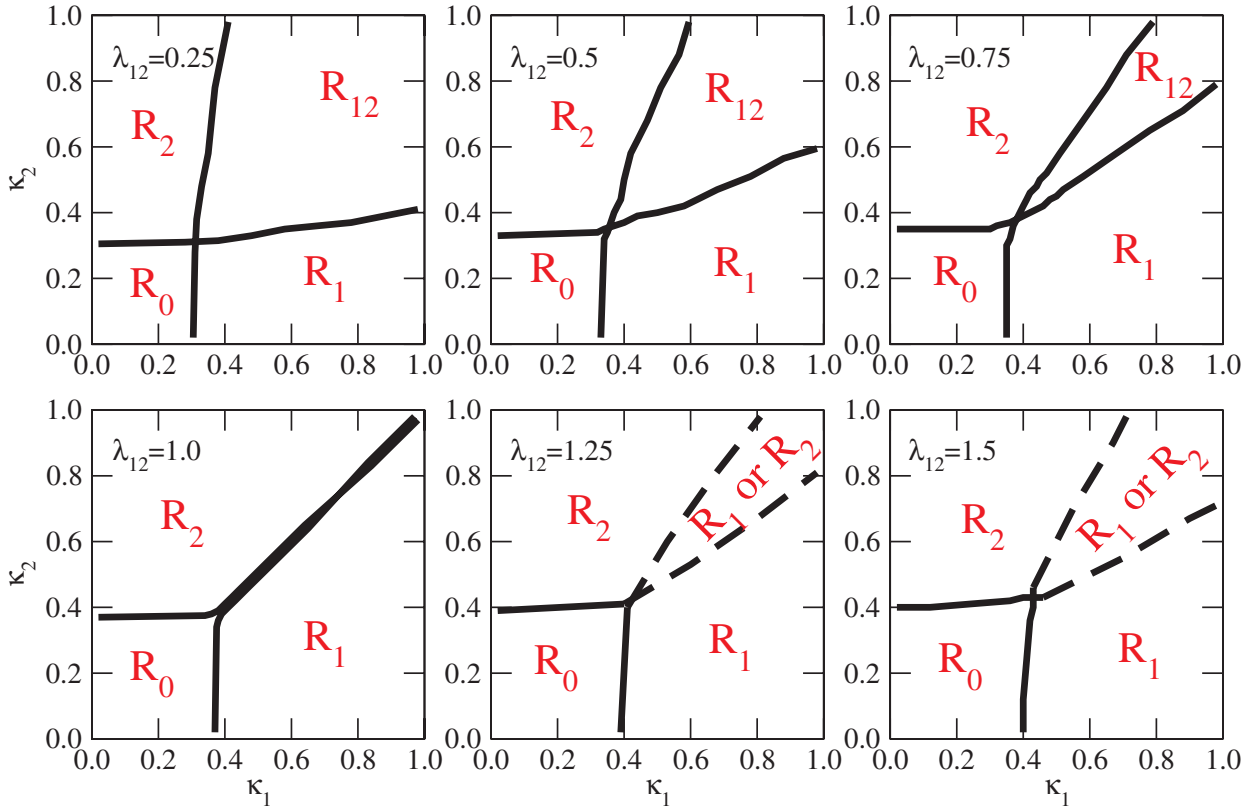

FIG. 7 (color online). Phase diagram for the theory with $\lambda_1 = \lambda_2 = 1$ at $\beta = 8.0$, as computed for six different λ_{12} values. R_{12} is the broken-symmetry region where L_{12} of Eq. (33) is nonzero, region R_1 has large L_{11}, region R_2 has large L_{22}, and region R_0 has small L_{11} and L_{22}. For $\lambda_{12} > 1$, hysteresis is observed in lieu of symmetry breaking.

As λ_{12} is increased beyond 1, the phase of broken intra-doublet symmetry vanishes and a region of hysteresis emerges, bounded in Fig. 7 by dashed lines. Only one, not both, of the scalar fields is in its Higgs phase in the region between the dashed lines, meaning that the phenomenology of this region is similar to either the R_1 region or the R_2 region. Which of these options is realized between the dashed lines depends upon how the dynamical system enters the region. For example, if κ_1 is gradually increased to pass through that region, then there will be no qualitiative change in our standard suite of observables as the system enters the region, but there will be a qualitative change as the system exists from the region (by crossing the second dashed line).

IV. SPONTANEOUS SYMMETRY BREAKING

A. Qualitative features

The simulations discussed above found large fluctuations (for sufficiently large κ_1 and κ_2 values) for the ensemble averages of $\mathrm{Re}(\Phi_1^\dagger(x)\Phi_2(x))$, $\mathrm{Im}(\Phi_1^\dagger(x)\Phi_2(x))$, $\mathrm{Re}(\Phi_1^\dagger(x)\Phi_{c2}(x))$ and $\mathrm{Im}(\Phi_1^\dagger(x)\Phi_{c2}(x))$. The sum of the squares of these four quantities is observed to have small fluctuations for all κ_1, κ_2 values, and is close to zero for small κ_1, κ_2 but far from zero for large κ_1, κ_2.

The large fluctuations become smaller when an explicit symmetry-breaking term, such as

$$\delta\mathcal{L} = \frac{\eta}{2}\,\mathrm{Tr}(\varphi_1^\dagger(x)\varphi_2(x)), \tag{35}$$

is added to the theory. Simulations can be performed for various values of η and then extrapolated to $\eta = 0$. For nonzero η, one finds $\langle \mathrm{Re}(\Phi_1^\dagger(x)\Phi_2(x))\rangle \neq 0$ but the other three ensemble averages are statistically zero, and $\langle \mathrm{Re}(\Phi_1^\dagger(x)\Phi_2(x))\rangle$ itself approaches zero as $\eta \to 0$.

To determine which symmetry-group generators are broken, consider how these ensemble averages are affected by the general symmetry transformation of Eqs. (26) and (27). In particular, the use of

$$\langle \mathrm{Im}(\Phi_1^\dagger\Phi_2)\rangle = \langle \mathrm{Re}(\Phi_1^\dagger\Phi_{c2})\rangle = \langle \mathrm{Im}(\Phi_1^\dagger\Phi_{c2})\rangle = 0 \tag{36}$$

leads to

$$\langle \Phi_1^\dagger\Phi_2\rangle \to (\cos\gamma_1\cos\gamma_2 e^{i(\alpha_2-\alpha_1)} + \sin\gamma_1\sin\gamma_2 e^{i(\beta_2-\beta_1)}) \times \langle \mathrm{Re}(\Phi_1^\dagger\Phi_2)\rangle, \tag{37}$$

$$\begin{aligned}\langle \Phi_1^\dagger\Phi_{c2}\rangle \to\ & e^{-2i\theta}\sin\gamma_{12}\cos\gamma_{12}\langle\Phi_2^\dagger\Phi_2 - \Phi_1^\dagger\Phi_1\rangle \\ & + e^{-2i\theta}[-\sin^2\gamma_{12}\sin\gamma_1\cos\gamma_2 e^{i(\alpha_2+\beta_1)} \\ & - \cos^2\gamma_{12}\cos\gamma_1\sin\gamma_2 e^{-i(\alpha_1+\beta_2)} \\ & + \sin^2\gamma_{12}\cos\gamma_1\sin\gamma_2 e^{i(\alpha_1+\beta_2)} \\ & + \cos^2\gamma_{12}\sin\gamma_1\cos\gamma_2 e^{-i(\alpha_2+\beta_1)}] \\ & \times \langle \mathrm{Re}(\Phi_1^\dagger\Phi_2)\rangle.\end{aligned} \tag{38}$$

Begin with the situation where the original global symmetry was only SU(2) × SU(2). As noted in the previous section, this corresponds to $\gamma_{12} = 0$. Therefore Eqs. (37) and (38) are simply

$$\langle \Phi_1^\dagger\Phi_2\rangle \to (\cos\gamma_1\cos\gamma_2 e^{i(\alpha_2-\alpha_1)} + \sin\gamma_1\sin\gamma_2 e^{i(\beta_2-\beta_1)}) \times \langle \mathrm{Re}(\Phi_1^\dagger\Phi_2)\rangle, \tag{39}$$

$$\langle \Phi_1^\dagger\Phi_{c2}\rangle \to 0. \tag{40}$$

The maximal unbroken subgroup is obtained from the case of $(\alpha_1, \beta_1, \gamma_1) = (\alpha_2, \beta_2, \gamma_2)$, which identifies a residual global SU(2). Therefore

$$\begin{aligned}&\mathrm{SU}(2)\times\mathrm{SU}(2) \to \mathrm{SU}(2) \\ &\text{if } (\kappa_1 = \kappa_2, \lambda_1 = \lambda_2 = \lambda_{12}) \text{ is not true.}\end{aligned} \tag{41}$$

Now consider Eqs. (37) and (38) in the special case where the original global symmetry was SU(2) × SU(2) × U(1) × U(1). Now $\gamma_{12} \neq 0$, but again the largest unbroken subgroup is obtained from the case of $(\alpha_1, \beta_1, \gamma_1) = (\alpha_2, \beta_2, \gamma_2)$, which gives

$$\langle \Phi_1^\dagger\Phi_2\rangle \to \langle \mathrm{Re}(\Phi_1^\dagger\Phi_2)\rangle, \tag{42}$$

$$\langle \Phi_1^\dagger\Phi_{c2}\rangle \to e^{-2i\theta}\sin\gamma_{12}\cos\gamma_{12}\langle\Phi_2^\dagger\Phi_2 - \Phi_1^\dagger\Phi_1\rangle. \tag{43}$$

As will be discussed below, lattice simulations find $\langle\Phi_2^\dagger\Phi_2\rangle \neq \langle\Phi_1^\dagger\Phi_1\rangle$. Therefore $\gamma_{12} = n\pi/2$ for some integer n, and θ remains as a symmetry generator in the theory. As a consequence, the symmetry breaking in this special case is

$$\begin{aligned}&\mathrm{SU}(2)\times\mathrm{SU}(2)\times\mathrm{U}(1)\times\mathrm{U}(1) \to \mathrm{SU}(2)\times\mathrm{U}(1) \\ &\text{if } (\kappa_1 = \kappa_2, \lambda_1 = \lambda_2 = \lambda_{12}) \text{ is true.}\end{aligned} \tag{44}$$

B. Symmetry-breaking order parameter

The calculations of the previous section can give qualitative information about the phase diagram, but getting a quantitative estimate of the order parameter in the broken phase requires a different approach. The system has to be forced to choose between different degenerate vacua by inserting an explicit symmetry-breaking term such as Eq. (35) into the theory and then studying the limit as the coefficient, η, approaches zero. The infinite-volume limit should be taken before removing the symmetry-breaking term.

Results of numerical simulations on finite size (12^4 and 20^4) lattices are displayed in Fig. 8. For hopping parameters below the phase transition (i.e. $\kappa < \kappa_c$), the symmetry-breaking vev extrapolates linearly to zero as η vanishes. For hopping parameters above the phase transition ($\kappa > \kappa_c$), the symmetry-breaking vev appears to extrapolate to nonzero values, except for a bending toward zero at small η (visible in the 12^4 simulation). This decrease reflects the

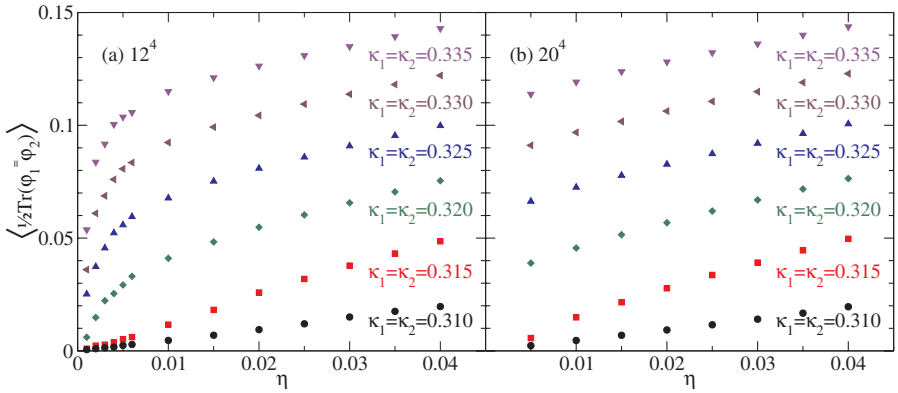

FIG. 8 (color online). A vacuum expectation value that breaks SU(2) × SU(2) is graphed as a function of its Lagrangian coefficient. These data are from simulations for the fixed-length theory with $\beta = 8$ on (a) 12^4 and (b) 20^4 lattices.

fact that there is no true spontaneous symmetry breaking in a finite system and is due to modes whose Compton wavelength becomes larger than the lattice size at small η. As the volume is increased this effect is restricted to a smaller region near $\eta = 0$.

To deal with the volume effect, we recall that the effective field theory in finite volume for a scalar theory in the broken phase was developed long ago [41,42] and was studied numerically in some detail for the one-doublet model [43].

Doing calculations of $\langle \frac{1}{2} \mathrm{Tr} \varphi_1^\dagger \varphi_2 \rangle$ for different volumes (from 8^4 to 20^4) and different η and using procedures which are verified by study of the one-doublet model, we can estimate the infinite-volume value of the order parameter. Figure 9 shows the value of the order parameter for the SU(2) × SU(2) symmetry breaking in two cases: the fixed-length theory and the theory with $\lambda_1 = \lambda_2 = \lambda_{12} = 1$. Using a parametrization $\langle \frac{1}{2} \mathrm{Tr} \varphi_1^\dagger \varphi_2 \rangle \propto (\kappa - \kappa_c)^\nu$ for $\kappa > \kappa_c$ we can estimate the critical κ. The values of κ_c corresponding to the lines in Fig. 9 are 0.316 for the fixed-length theory and 0.365 for $\lambda_1 = \lambda_2 = \lambda_{12} = 1$.

Recall the prediction from Eq. (44) of an extra broken U(1) symmetry in the theory when $\kappa_1 = \kappa_2$ and $\lambda_1 = \lambda_2 = \lambda_{12}$. This is verified by adding a symmetry-breaking term to the theory, and then extrapolating its coefficient to zero. In fact, the simplest way to add an appropriate extra term is to run simulations with $\kappa_1 \neq \kappa_2$ and extrapolate the results to $\kappa_1 = \kappa_2$. An example is provided in Fig. 10. The transition from broken to unbroken U(1) is found to occur at the same critical hopping parameter as the breaking of the SU(2) × SU(2). At first glance, the kink in the $\kappa_1 = 0.48$ curve of Fig. 10 may be puzzling, but comparison to Fig. 7 makes the interpretation clear: the kink occurs at the phase transition crossed by varying κ_2 while holding κ_1 fixed.

C. Goldstone bosons

Spontaneous breaking of any continuous global symmetry generates a Goldstone boson for each broken generator. The three Goldstone bosons arising from SU(2) × SU(2) → SU(2) are found to couple readily to the operators

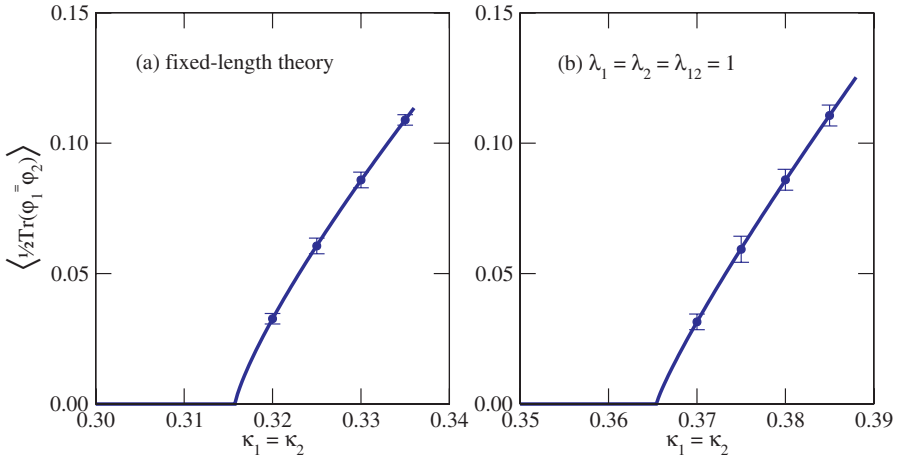

FIG. 9 (color online). An order parameter for SU(2) × SU(2) breaking after extrapolation to $\eta = 0$. These data are from simulations with $\beta = 8$.

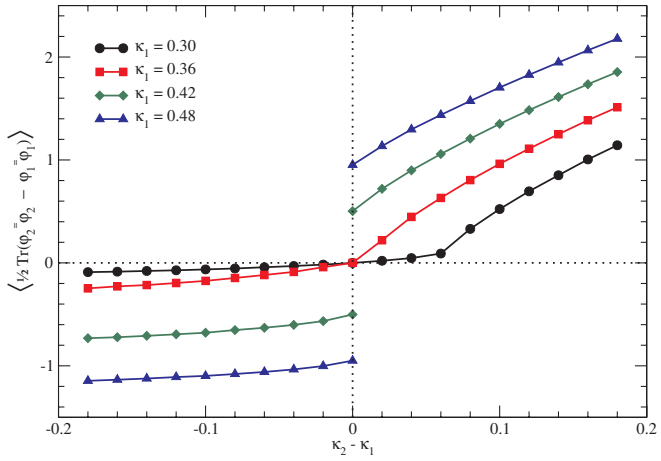

FIG. 10 (color online). An order parameter for spontaneous breaking of the extra U(1). These data are from simulations with $\beta = 8$ and $\lambda_1 = \lambda_2 = \lambda_{12} = 1$.

$$\frac{1}{2}\,\mathrm{Tr}[\varphi_1^\dagger \varphi_2 \tau_a] \tag{45}$$

where τ_1, τ_2 and τ_3 are the standard Pauli matrices. These operators are invariant under the unbroken global SU(2) and under the gauge symmetry (which is never broken). Examples of correlators for a range of η are shown in Fig. 11 and the corresponding squared masses are shown in Fig. 12. The small statistical errors provide convincing evidence that the Goldstone boson squared mass vanishes with a linear extrapolation of $\eta \to 0$. For comparison, the graph also contains results for the operator

$$\frac{1}{2}\,\mathrm{Tr}[\varphi_1^\dagger \varphi_2]. \tag{46}$$

That operator is not an SU(2) triplet and does not couple to the Goldstone bosons, but it does provide evidence of a heavy scalar particle in the theory. One might wish to name

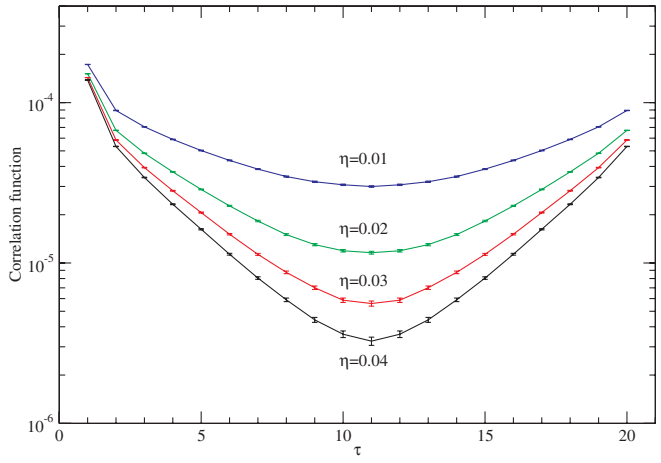

FIG. 11 (color online). Correlation functions for the operators defined in Eq. (45). These data are from simulations on $16^3 \times 20$ lattices with $\beta = 8$ in the fixed-length theory.

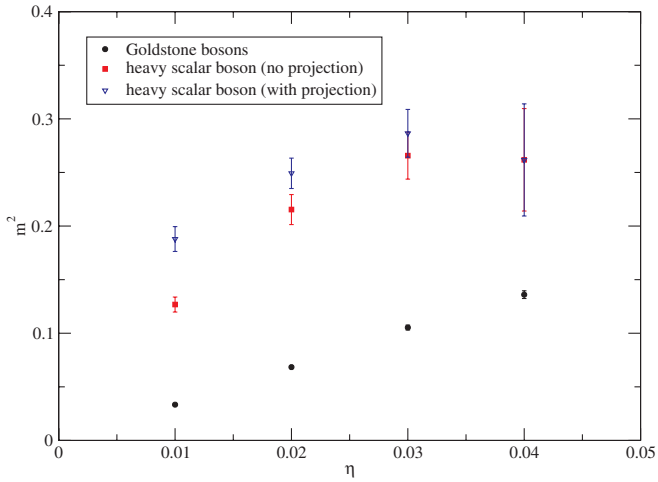

FIG. 12 (color online). Squared masses for the Goldstone bosons obtained from Eq. (45) and the scalar boson obtained from Eq. (46). These data are from simulations on $16^3 \times 20$ lattices with $\beta = 8$ in the fixed-length theory.

the Goldstone bosons π_a and the extra scalar boson "σ" to follow familiar notational conventions. In addition to the direct method for obtaining the σ correlation function, the projection method described in [43] was also used. This projection is given by

$$\mathcal{O}_{\mathrm{proj}} = \sum_{a=1}^{3} \frac{M_a}{|M|}\,\frac{1}{2}\,\mathrm{Tr}[\varphi_1^\dagger \varphi_2 \tau_a] \tag{47}$$

where, on a lattice with N sites,

$$M_a = \frac{1}{N}\sum_x \frac{1}{2}\,\mathrm{Tr}[\varphi_1^\dagger \varphi_2 \tau_a], \tag{48}$$

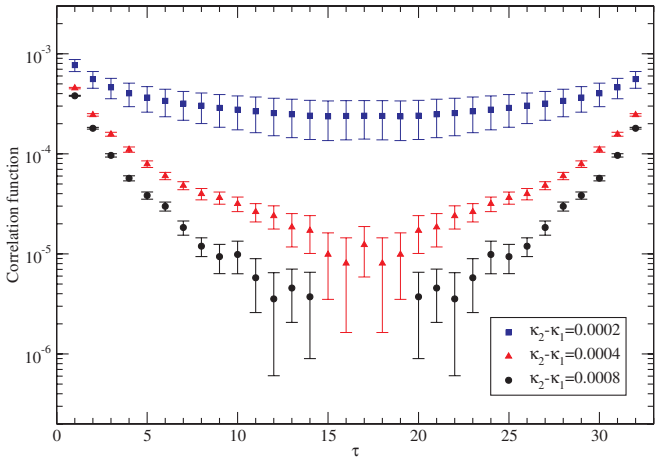

FIG. 13 (color online). Correlation functions for the operator obtained from Eq. (50). These data are from simulations on $16^3 \times 32$ lattices with $\beta = 2$, $\kappa_1 = 0.48$ and $\lambda_1 = \lambda_2 = \lambda_{12} = 1$.

$$|M| = \sqrt{M_1^2 + M_2^2 + M_3^2}. \quad (49)$$

A possible operator for producing the Goldstone boson associated with the breaking of an extra U(1) symmetry present when ($\kappa_1 = \kappa_2$, $\lambda_1 = \lambda_2 = \lambda_{12}$) is

$$\frac{1}{2}\,\mathrm{Tr}[\varphi_1^\dagger \varphi_1 - \varphi_2^\dagger \varphi_2]. \quad (50)$$

Numerical simulations using this operator produced sizable statistical fluctuations as shown in Fig. 13, but are consistent with a mass that vanishes as $\eta \to 0$.

V. SUMMARY

In this paper we studied an SU(2) Higgs model using lattice field theory methods. This approach provides a view of symmetry breaking which is different from the one familiar from the usual perturbative treatment of the standard model. The difference stems from the use of the gauge field link in the lattice formulation. This removes the requirement of gauge fixing and allows all quantities to be calculated in a gauge-invariant way. The physical states of the theory are described by gauge-invariant operators which are necessarily composite. The lattice Higgs model is in this sense not unlike QCD.

The SU(2) lattice Higgs model with one scalar doublet was studied long ago. Regions of parameter space with seemingly different physical behavior were identified by examining the scalar and vector particle spectrum. These were associated with confined and Higgs "phases." However, it was suggested that in fact the model with only one fundamental scalar doublet has only one phase and no symmetries, local or global, are broken. Numerical simulations are in accord with this expectation. The low-lying spectrum of the theory consists of a massive scalar boson and a degenerate triplet of massive vector bosons.

The addition of a second scalar doublet can lead to a richer symmetry structure than in the one-doublet model. For the model studied in this paper the global symmetry is generically $SU(2) \times SU(2)$ but is enlarged to $SU(2) \times SU(2) \times U(1) \times U(1)$ for particular parameter choices which allow for symmetry under interdoublet mixing. By examining the vacuum expectation values of a variety of operators, the phase diagram was mapped out. The confined and Higgs regions associated with the individual doublets could be identified. When the hopping parameters are sufficiently large a new phase, in which there is a strong correlation of the two doublet fields and the global symmetry is spontaneously broken, emerges.

The spontaneous symmetry breaking was verified by calculation of the order parameter for some specific choices of the model parameters. This was done by the usual procedure of introducing an explicit symmetry-breaking term and studying the behavior of the system as the volume of the simulation was increased and the symmetry-breaking term was removed. The presence of Goldstone bosons in the broken phase was verified by calculation of the correlation functions of appropriate gauge-invariant interpolating operators. In addition to Goldstone bosons we also find scalar states which remain massive in all phases. As in the one-doublet model the gauge symmetry is unbroken.

The focus of this work was spontaneous global symmetry breaking so the question of the spectrum of vector bosons was not addressed. In the nonperturbative lattice approach the vector bosons are composite particles and are expected to be massive in all regions of the phase diagram. This can be confirmed by a cursory examination of the correlation functions of the vector operators. However, the quantitative determination of the mass is a difficult problem due to the plethora of operators that can be constructed which would require careful study of operator mixing and also decays due to the presence of light (pseudo-)Goldstone bosons in the theory. Such a study might give some information about the nature of the theory in different regions of the parameter space. Work on the three-dimensional Higgs model [44] gives some insight into the difficulty and benefit of a spectrum calculation.

ACKNOWLEDGMENTS

This work was supported in part by the Natural Sciences and Engineering Research Council of Canada, and by computing resources of the Shared Hierarchical Academic Research Computing Network [45].

[1] M. Sher, Phys. Rep. **179**, 273 (1989).
[2] R. Barbieri, L. J. Hall, and V. S. Rychkov, Phys. Rev. D **74**, 015007 (2006).
[3] E. Ma, Phys. Rev. D **73**, 077301 (2006).
[4] R. Balian, J. M. Drouffe, and C. Itzykson, Phys. Rev. D **10**, 3376 (1974).
[5] S. Elitzur, Phys. Rev. D **12**, 3978 (1975).
[6] G. F. De Angelis, D. de Falco, and F. Guerra, Phys. Rev. D **17**, 1624 (1978).
[7] J. Fröhlich, G. Morchio, and F. Strocchi, Nucl. Phys. **B190**, 553 (1981).
[8] E. H. Fradkin and S. H. Shenker, Phys. Rev. D **19**, 3682 (1979).
[9] K. Osterwalder and E. Seiler, Ann. Phys. (N.Y.) **110**, 440 (1978).
[10] C. B. Lang, C. Rebbi, and M. Virasoro, Phys. Lett. B **104**,

294 (1981).
[11] E. Seiler, Lect. Notes Phys. **159**, 1 (1982).
[12] H. Kuhnelt, C. B. Lang, and G. Vones, Nucl. Phys. **B230**, 16 (1984).
[13] I. Montvay, Phys. Lett. B **150**, 441 (1985).
[14] J. Jersák, C. B. Lang, T. Neuhaus, and G. Vones, Phys. Rev. D **32**, 2761 (1985).
[15] H. G. Evertz, J. Jersák, C. B. Lang, and T. Neuhaus, Phys. Lett. B **171**, 271 (1986).
[16] V. P. Gerdt, A. S. Ilchev, V. K. Mitrjushkin, I. K. Sobolev, and A. M. Zadorozhnyi, Nucl. Phys. **B265**, 145 (1986).
[17] W. Langguth, I. Montvay, and P. Weisz, Nucl. Phys. **B277**, 11 (1986).
[18] I. Montvay, Nucl. Phys. **B269**, 170 (1986).
[19] H. G. Evertz, E. Katznelson, P. Lauwers, and M. Marcu, Phys. Lett. B **221**, 143 (1989).
[20] A. Hasenfratz and T. Neuhaus, Nucl. Phys. **B297**, 205 (1988).
[21] K. Jansen, Nucl. Phys. B, Proc. Suppl. **47**, 196 (1996).
[22] K. Rummukainen, Nucl. Phys. B, Proc. Suppl. **53**, 30 (1997).
[23] M. Laine and K. Rummukainen, Nucl. Phys. B, Proc. Suppl. **73**, 180 (1999).
[24] Z. Fodor, Nucl. Phys. B, Proc. Suppl. **83**, 121 (2000).
[25] G. Bhanot, K. Bitar, U. M. Heller, and H. Neuberger, Nucl. Phys. **B353**, 551 (1991); **B375**, 503(E) (1992).
[26] K. Holland and J. Kuti, Nucl. Phys. B, Proc. Suppl. **129**, 765 (2004).
[27] K. Holland, Nucl. Phys. B, Proc. Suppl. **140**, 155 (2005).
[28] J. Shigemitsu, Nucl. Phys. B, Proc. Suppl. **20**, 515 (1991).
[29] A. K. De and J. Jersák, Adv. Ser. Dir. High Energy Phys. **10**, 732 (1992).
[30] J. Giedt and E. Poppitz, J. High Energy Phys. 10 (2007) 076.
[31] Z. Fodor, K. Holland, J. Kuti, D. Nogradi, and C. Schroeder, Proc. Sci., LAT2007 (2007) 056.
[32] P. Gerhold and K. Jansen, J. High Energy Phys. 09 (2007) 041; 10 (2007) 001; 07 (2009) 025; 04 (2010) 094.
[33] M. Wurtz, R. Lewis, and T. G. Steele, Phys. Rev. D **79**, 074501 (2009).
[34] C. Bonati, G. Cossu, M. D'Elia, and A. Di Giacomo, Nucl. Phys. **B828**, 390 (2010).
[35] I. Campos, Nucl. Phys. **B514**, 336 (1998).
[36] W. Langguth and I. Montvay, Phys. Lett. B **165**, 135 (1985).
[37] B. Bunk, Nucl. Phys. B, Proc. Suppl. **42**, 566 (1995).
[38] Z. Fodor and K. Jansen, Phys. Lett. B **331**, 119 (1994).
[39] Z. Fodor, J. Hein, K. Jansen, A. Jaster, and I. Montvay, Nucl. Phys. **B439**, 147 (1995).
[40] J. Greensite and S. Olejnik, Phys. Rev. D **74**, 014502 (2006).
[41] P. Hasenfratz and H. Leutwyler, Nucl. Phys. **B343**, 241 (1990).
[42] A. Hasenfratz, K. Jansen, J. Jersák, H. A. Kastrup, C. B. Lang, H. Leutwyler, and T. Neuhaus, Nucl. Phys. **B356**, 332 (1991).
[43] A. Hasenfratz, K. Jansen, J. Jersák, C. B. Lang, T. Neuhaus, and H. Yoneyama, Nucl. Phys. **B317**, 81 (1989).
[44] O. Philipsen, M. Teper, and H. Wittig, Nucl. Phys. **B528**, 379 (1998).
[45] www.sharcnet.ca.